

Observations and modeling of the Antarctic phytoplankton crop in relation to mixing depth

B. GREG MITCHELL* and OSMUND HOLM-HANSEN†

(Received 5 January 1990; in revised form 19 October 1990; accepted 23 October 1990)

Abstract—The multi-disciplinary program RACER (Research on Antarctic Coastal Ecosystem Rates) conducted eight surveys of a 69-station grid in a 100×250 km area in the southwestern Bransfield Strait from December 1986 to March 1987. Mean phytoplankton crop size in the upper 50 m during December, January, February and March was 291, 176, 58 and 50 mg Chl *a* m^{-2} , respectively, and was inversely proportional to the increasing mean depth of the upper mixed layer (UML) (15, 17, 26 and 30 m, respectively). Massive mid-summer phytoplankton blooms (>10 mg Chl *a* + phaeo m^{-3}) were persistent nearshore where we observed shallow UMLs (<20 m) caused by meltwater stabilization ($\Delta\sigma_t$ 0.25–1.0 from 0 to 75 m). Drake Passage waters were low in phytoplankton biomass (<1.0 mg Chl *a* + phaeo m^{-3}), and had deep UMLs (>20 m) with small density gradients ($\Delta\sigma_t$ 0.05–0.20 from 0 to 75 m). Proximity to stabilizing meltwater and protection from intense Antarctic storm activity appear to be essential for the development of persistent massive blooms. A model of Antarctic phytoplankton growth based on mixing depth and pigment-specific light attenuation and *in situ* photosynthesis–irradiance relationships indicates that the depth of the UML (Z_{UML}) can be used to predict the upper limit of the phytoplankton crop size. Observed phytoplankton biomass for diverse Southern Ocean ecosystems is discussed in relation to the mean light level of the UML, growth and loss rates of Antarctic phytoplankton, and the depth and duration of stratification required before a bloom ensues. Assuming nutrients do not limit the crop size, a best-fit to observations indicates specific loss rates must be approximately 0.3 – 0.35 day^{-1} and massive blooms occur only if $Z_{UML} < 25$ m. The grazing component of this predicted loss rate is higher than previously estimated. We conclude that grazing rates are greater than previously reported, or vertical flux rates of nutrients limit massive blooms.

INTRODUCTION

ANTARCTIC waters are unique in that concentrations of inorganic nutrients are very high, yet phytoplankton standing stocks and rates of primary production are generally low (~ 0.4 mg Chl *a* m^{-3} and 0.1 – 0.3 g C m^{-2} day^{-1} , respectively). The condition of low biomass in spite of high nutrients has often been referred to as a major “paradox” of the Southern Ocean (EL-SAYED, 1987). There are exceptions to this generality, and massive blooms (>10 mg Chl *a* + phaeo m^{-3}) have been observed in some restricted regions. In fact, nutrient depletion (<1 mmol NO_3 m^{-3}) in surface waters of blooms has been reported for ice-edge (NELSON and SMITH, 1986) and coastal (HOLM-HANSEN *et al.*, 1989)

*Marine Research Division, Scripps Institution of Oceanography, University of California, La Jolla, CA 92093-0218, U.S.A.

†Polar Research Program, Scripps Institution of Oceanography, University of California, La Jolla, CA 92093-0202, U.S.A.

ecosystems. Primary production in the Antarctic supports a large secondary and tertiary production, and may be an important sink for atmospheric CO₂. In order to assess the primary production potential of the Antarctic planktonic ecosystem, it is crucial to understand both the reasons for low biomass under apparently replete nutrient conditions and the mechanisms of massive bloom formation and decline.

Many researchers have speculated on the factors responsible for causing the apparent nutrient-biomass "paradox". Light, temperature, trace-nutrients, grazing, and physical mixing processes have all been commonly invoked as key factors. A compelling new hypothesis (MARTIN and FITZWATER, 1988; MARTIN *et al.*, 1990) postulates that iron from coastal and ice-edge sources is used up in blooms close to the source and the open Southern Ocean has a very limited atmospheric supply of trace nutrients. HART (1934) argued that physical mixing processes are the dominant factor that control the distribution and abundance of phytoplankton in Antarctic waters. The depth of mixing will determine the mean light level available for phytoplankton photosynthesis. Most researchers who have been concerned with this problem concur with this early diagnosis of Hart's, and refer to the treatment of the subject by SVERDRUP (1953). Sverdrup, however, used data from the Norwegian Sea to formulate the concept that depth of mixing controls phytoplankton abundance, and he used assumptions regarding photosynthetic and respiratory rates to estimate the "critical" depth of mixing. Knowledge of the critical depth for net production is useful but cannot be used directly to estimate the net accumulation of biomass for mixing conditions which allow growth of the crop. Besides phytoplankton physiology, a realistic estimate of biomass accumulation requires an estimate of sinking and grazing losses. Little is known about respiratory rates of Antarctic phytoplankton or their loss due to other factors such as grazing and sinking. New insights have been made recently regarding the various controlling factors restraining the phytoplankton crop including respiration (TILZER and DUBINSKY, 1987; SAKSHAUG *et al.*, 1991), grazing (BOYD *et al.*, 1984; SCHNACK *et al.*, 1985; HUNTLEY *et al.*, 1991) sinking (JOHNSON and SMITH, 1986; VON BODUNGEN *et al.*, 1986; KARL *et al.*, 1991) and mean wind speed (CLARKE *et al.*, 1988).

It is now appropriate to evaluate the relationship between depth of mixing, photosynthetically available radiation (PAR), and phytoplankton biomass in Antarctic waters from a combined theoretical and empirical basis. Data on Antarctic planktonic ecosystems may now be adequate to provide insight to the relationship between depth of the upper mixed layer (Z_{UML}), the strength of stratification and the maximal concentration of phytoplankton biomass that can be developed. Understanding the coherence between physical and biological processes is problematic in Antarctic waters where it is logistically difficult to obtain the detailed temporal and spatial coverage required to test hypotheses. It is often possible to use models to simulate the environment in order to test specific hypotheses which cannot be tested with the limited spatial and temporal observational database of field programs. It is still essential, however, to have an appropriate database, such as that collected during the RACER program, with which to validate the predictions of the model.

In other papers we described the distribution of phytoplankton biomass and production with time over the RACER sampling grid (HOLM-HANSEN and MITCHELL, 1991) and the relationship between biomass and light attenuation coefficients (MITCHELL and HOLM-HANSEN, 1991). Observed rate processes in those papers, including light-specific rates of primary production and pigment-specific attenuation coefficients, were used to develop a model which predicts the maximum size of the phytoplankton crop as a function of mixing

depth, surface irradiance and losses due to respiration, grazing and sinking. Rates of carbon sedimentation have been measured (KARL *et al.*, 1991) and are used together with the model to estimate grazing losses. A fit of the model to observations from RACER and diverse Antarctic literature allows the predictions of carbon:Chl *a* ratios, grazing and sinking losses, and the rate of vertical nutrient resupply required to develop and sustain massive phytoplankton blooms.

MATERIALS AND METHODS

Sampling protocol

Data were acquired at 69 stations in Bransfield Strait and contiguous waters of Gerlache Strait and Drake Passage (Fig. 1) during the "fast" cruise each month from December 1986 to March 1987. Immediately following each "fast" cruise, more intensive studies were done at 25 of the stations during a 10-day "slow" cruise. *In situ* rate processes, including primary production (HOLM-HANSEN and MITCHELL, 1991) and particle flux (KARL *et al.*, 1991) were measured each month at five stations (Fig. 1). Further details regarding the sampling program are described by HUNTLEY *et al.* (1991).

At each station a profiling system was deployed between the surface and 200 m for continuous recording of physical, optical and biological parameters. This profiling unit consisted of a General Oceanics rosette equipped with the sensors listed below and ten 10-liter PVC Niskin bottles with teflon-covered springs. Sensors on the profiling unit included temperature and conductivity (Sea Bird Electronics, Inc.), a 0.25 m path length transmissometer (Sea Tech, Inc.), a flash-lamp fluorometer (Sea Tech, Inc.), and a MER 1012-F optical unit (Biospherical Instruments Inc.) for recording of depth, PAR, seven channels of downwelling spectral irradiance and five channels of upwelling spectral radiance. Signals from all underwater sensors were transmitted over a standard single conductor oceanographic cable to shipboard computers where the data were stored and also displayed on a video screen in real time.

The physical oceanographic data have been described by NIELER *et al.* (1991), who provided us with profiles of temperature, salinity, and water density at the RACER stations. In general, salinity, temperature (therefore density) and biological properties were uniformly distributed in an upper mixed layer (UML). These data were used to determine the depth of the upper mixed layer (Z_{UML}) at a resolution of 5 m. An objective and a subjective method were used to define the Z_{UML} . An objective computation method used a 5 m window to search for a change in $\sigma_t \geq 0.05$ over the 5 m interval. When this criterion was met, the shallower depth of the window was defined as Z_{UML} . A separate subjective determination was made by examination of plots and printouts of temperature, salinity, density and beam transmission. In general, the two approaches agreed within 5 m. Discrepancies were primarily due to subjective determinations of Z_{UML} shallower than the objective determination caused by temperature stratification which was insufficient to change σ_t by the objective criterion. In these cases, the subjectively determined Z_{UML} was used if the temperature change was $\geq 0.05^\circ\text{C}$.

Water samples for chlorophyll *a* (Chl *a*) and phaeopigment analysis (50–100 ml) were filtered at a vacuum differential of <20 cm Hg through 25 mm glass fiber filters (Whatman, GF/F). Pigments on the filter were extracted in 10 ml absolute methanol (HOLM-HANSEN and RIEMANN, 1978) and the Chl *a* and phaeopigment concentrations were determined by

measurement of fluorescence (HOLM-HANSEN *et al.*, 1965) in a Turner Designs fluorometer. The fluorometer was calibrated against HPLC purified Chl *a*. Stability of the calibration factors was checked daily by the use of a coproporphyrin standard (COP-I-5, Sigma Chemical Co.).

Details of the *in situ* primary production estimates are found in HOLM-HANSEN and MITCHELL (1991). Details of the sediment trap methods are found in KARL *et al.* (1991). Samples for estimates of the flux of Chl *a* were obtained from non-preserved, dark traps.

A model of light-dependent production

A simple model of light-dependent photosynthesis was developed based on empirical observations from the RACER database. Table 1 summarizes the definitions of symbols and parameters used in the model and elsewhere in the paper. Nutrient limitation was not included since concentrations of macronutrients have generally been observed to be in

Table 1. Definitions of terms used in the text

α	Initial slope of P-I relationship
c	Speed of sound in water
C_d	Drag coefficient of air-water interface
C:Chl <i>a</i>	Ratio of carbon to Chl <i>a</i> for phytoplankton (w/w)
C:N	Molar ratio of phytoplankton carbon to nitrogen
[Chl] ₀ , [Chl] _{<i>t</i>}	Chl <i>a</i> concentration at time = 0 and time = <i>t</i>
dChl <i>a</i>	Daily change in Chl <i>a</i> concentration of UML
E_{UML}	Stability of pycnocline below the UML
g	Gravitational acceleration
K_{PAR}	Diffuse attenuation coefficient for PAR
k_z	Vertical diffusivity coefficient
l	Specific loss rate of phytoplankton
m_0	Mixing efficiency coefficient
μ	Specific growth rate of phytoplankton
[NO ₃], [NO ₃] ₀	Nitrate concentration, initial nitrate concentration
PAR	Photosynthetically available radiation
PAR(0 ⁺)	Downwelling PAR at the sea surface
P_c	Hourly rate of carbon production
$P_c(UML)$	Daily mean carbon production of UML
PE	Potential energy of upper ocean
P_g	Phytoplankton biomass grazed by zooplankton
P_m	Maximum Chl <i>a</i> specific rate of production
ρ_a, ρ, ρ_0	Density of air, seawater, typical seawater
r, g_z, s	Specific rates of respiration, grazing and sinking
$s_c, s_{Chl a}$	Specific rates of sinking for carbon and Chl <i>a</i>
s_p	Specific rate of sinking for primary production
τ	Light transmittance of the air-sea interface
U_*	Friction velocity of air-sea interface
U_{wind}	Wind velocity at the sea surface
UML	Upper mixed layer of the ocean
Z_{UML}	Depth of the UML
z	Depth in the ocean
z_B	Lower limit of integration over depth

excess of the concentrations required for maximal growth (HOLM-HANSEN *et al.*, 1977; EL-SAYED *et al.*, 1983; NELSON and SMITH, 1986; but see MARTIN and FITZWATER, 1988). The accumulation of Chl *a* biomass through time (*t*) is described by

$$[\text{Chl } a]_t = [\text{Chl } a]_0 e^{(\mu - l)t}, \quad (1)$$

where $[\text{Chl } a]_0$ and $[\text{Chl } a]_t$ are the initial and final concentrations of Chl *a*. The difference between specific growth and loss rates of phytoplankton biomass, μ and l , respectively, determine the rate of accumulation or decline in the crop. The value of l is the sum of losses due to respiration (r), grazing (g_z) and sinking (s). In this simple model, the loss terms are aggregated and held constant during a 60-day run of the model. This is reasonable because very little is known about these specific rates, so it would be arbitrary to presume to model the time- or depth-based variations in these parameters in the absence of data to support the parameterizations. Alternatively, one may use a model based on parameters which are well described in order to estimate the magnitude of parameters which are poorly described. We believe that the loss rate terms are the least known parameters of the model.

A good description of the light-dependent rate of *in situ* primary production (HOLM-HANSEN and MITCHELL, 1991) is the basis for determining μ , as outlined below. The carbon-based rate of primary production P_c ($\text{mg C m}^{-3} \text{ h}^{-1}$) at any depth z within the UML is defined as

$$P_c(z) = [\text{Chl } a]_0 P_m (1 - e^{-(\alpha \text{PAR}(z)/P_m)}), \quad (2)$$

This model of production follows the formulation of PLATT and JASSBY (1976) and the parameters α ($0.06 \text{ mg C mg Chl } a^{-1} \text{ h}^{-1} (\mu \text{Ein m}^{-2} \text{ s}^{-1})^{-1}$) and P_m ($1.1 \text{ mg C mg Chl } a^{-1} \text{ h}^{-1}$) are the initial slope and maximum rate of the Chl *a* specific photosynthesis-irradiance (P-I) relationship. $\text{PAR}(z)$ is the photosynthetically available radiation at depth z . A best-fit of RACER data from over 140 *in situ* production measurements and the dose of PAR for each incubation was used to estimate α and P_m (HOLM-HANSEN and MITCHELL, 1991), hence the parameters are assumed to have no seasonal, depth, temperature or light dependence. Our value for P_m is similar to the value observed by BRIGHTMAN and SMITH (1989) for winter populations in the same region. Our value of α is higher than the values reported previously. P-I relationships were studied for phytoplankton (BRIGHTMAN and SMITH, 1989) and ice algae (PALMISANO *et al.*, 1985) using red-rich tungsten-halogen lamps. TILZER *et al.* (1985) used on-deck incubations and surface solar illumination in their work. Our values for α are based on *in situ* observations of production and PAR which is the most ecologically relevant method. Since the spectrum of PAR *in situ* is narrowed to blue-green irradiance which is optimal for phytoplankton (MITCHELL and HOLM-HANSEN, 1991), we would expect to observe a higher α than those measured using a red-rich quartz-halogen lamp or surface solar energy.

$\text{PAR}(z)$, the photosynthetically available radiation at depth z , is calculated in the model according to

$$\text{PAR}(z) = \text{PAR}(0^+) \tau e^{-K_{\text{PAR}} z}, \quad (3)$$

where $\text{PAR}(0^+)$ is the flux of PAR above the sea surface and τ is the transmittance of the air-sea interface. The value of τ was assumed to be 0.8 which is appropriate for low solar angles or diffuse skies (AUSTIN, 1974). The attenuation coefficient for PAR in the mixed layer, K_{PAR} , is well correlated to pigment concentrations as shown by MITCHELL and

HOLM-HANSEN (1991) (linear fit, $r^2 = 0.74$, $n = 130$). The best fit to the observations is used in the model

$$K_{PAR}(m^{-1}) = 0.078 + 0.0136[Chl\ a + phaeo\ mg\ m^{-3}]. \quad (4)$$

The constant $0.078\ m^{-1}$ is the attenuation due to water and materials which do not covary with Chl *a* + phaeo. Our value is higher than values for pure water reported elsewhere (e.g. $0.027\ m^{-1}$ reported by SMITH and BAKER, 1978). As argued effectively by MOREL (1988), previously reported low values of K_{PAR} for water are unreasonable in the upper 50 m due to narrowing of the spectral irradiance distribution of PAR with depth. MOREL (1988) reports a mean value of K_{PAR} for water of approximately $0.07\ m^{-1}$, depending on depth in the upper 50 m.

Phaeopigments are not explicitly included in the model; it is assumed that the attenuation coefficient of Chl *a* is similar to observed attenuation by Chl *a* + phaeo. Since we only model the response of the UML, where Chl *a* is constant with depth, K_{PAR} is assumed to have no depth dependence. The surface irradiance, $PAR(0^+)$ was measured continuously during the 4 months (December to March) of the RACER program (HOLM-HANSEN and MITCHELL, 1991). For the model, we assume the rate that $PAR(0^+)$ increases prior to the summer solstice is the same as the rate of decrease we observed from the summer solstice in December to the end of RACER in March. The daily change in Chl *a* concentration in the UML, $dChl\ a$, was calculated according to

$$dChl\ a = P_c(UML)/C:Chl\ a, \quad (5)$$

where $P_c(UML)$ is the daily mean carbon-based productivity over the entire mixed layer at the end of a growth day. Loss terms were applied at the end of each growth day so that $dChl\ a$ could be used to calculate the specific growth rate. The assumption that the UML has a uniform distribution of Chl *a* at the end of a growth day in spite of differential light-dependent rates of growth is justified based on the uniform vertical profiles of particulates typically observed in the UML (e.g. Fig. 2). The phytoplankton-specific growth rate for the UML is calculated according to

$$\mu(\text{day}^{-1}) = \ln([Chl\ a]_0 + dChl\ a)/[Chl\ a]_0. \quad (6)$$

From the above equations, it is evident that the specific growth rate of the phytoplankton in the UML will be a function only of the surface irradiance, depth of mixing, C:Chl *a* and the concentration of Chl *a* in the mixed layer. During runs of the model, the Z_{UML} and loss terms (r , g_z and s) are held constant for a 60-day period ending at the summer solstice. A 13-year record at Signy Island indicates that the spring bloom initiates in November and peaks within 60 days (CLARKE *et al.*, 1988). We observed massive blooms ($Chl\ a > 10\ mg\ m^{-3}$) in late November and early December 1988, on the shelf south of Anvers Island and in Gerlache Strait (data not presented here), suggesting that this bloom had been initiated at least a month before our cruise. Data in NIILER *et al.* (1991) indicate that the maximum rate of transport of a parcel of water across the RACER grid would be on the order of 15 days. However, the regions where we observed massive blooms generally occurred in water masses which appeared to have persistent eddy-like features. Drifter deployments during November 1989, in the same vicinity as the work reported here, indicate that the water mass in the northeastern Gerlache Strait can be confined within the Strait for greater than 90 days (NIILER *et al.*, in press). The model presented here is most relevant for water masses, like those of the northern Gerlache Strait, where horizontal advection may be

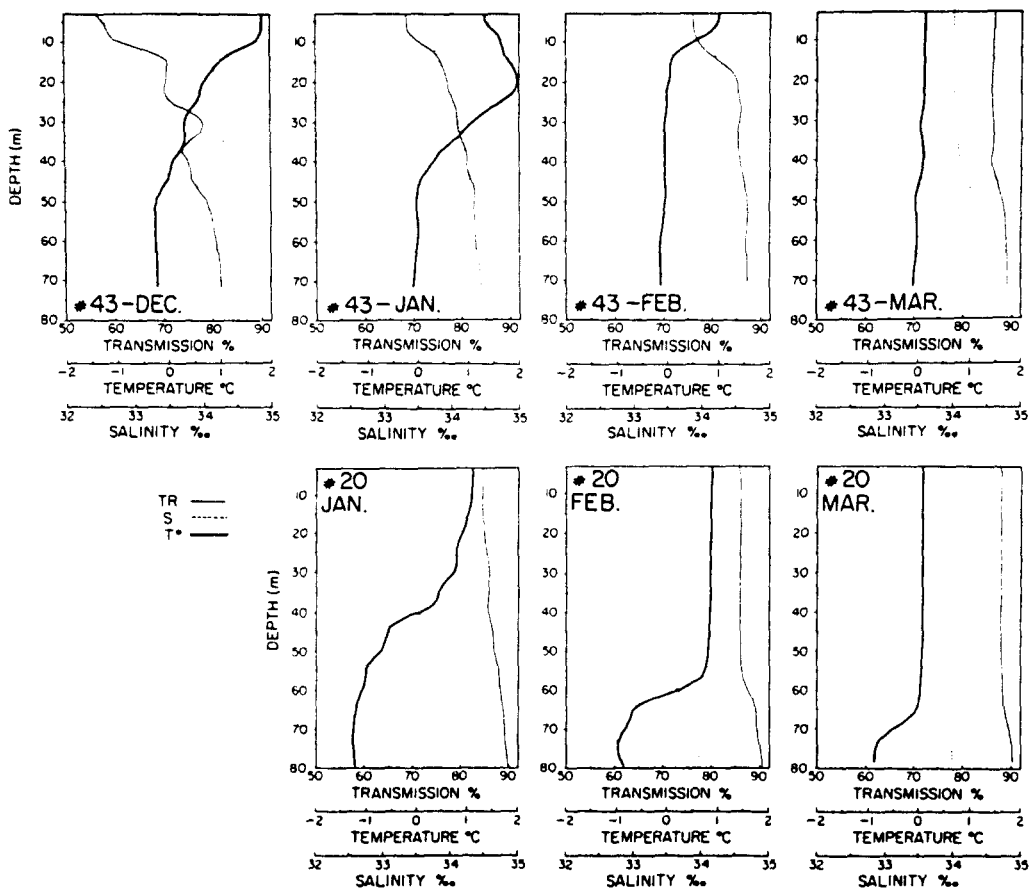


Fig. 2. Profiles of temperature, salinity and per cent light transmission (0.25 m path length) at Sta. 43 (Gerlache Strait) and Sta. 20 (Drake Passage), showing progressive changes from December to March. No data were obtained at Sta. 20 in December due to presence of sea ice. For all profiles presented: transmission, % (—); temperature, °C (—); salinity, ‰ (·····).

limited by persistent eddy-like circulation, or for open waters where horizontal transport in a relatively invariant meteorological and topographical field has little influence on vertical features or phytoplankton distributions. Complex flow and frontal mixing in Bransfield Strait may be less amenable to the type of model presented here.

For all runs, the molar ratio of carbon to nitrogen (C:N mole:mole) was 6.6 (REDFIELD *et al.*, 1963; NELSON *et al.*, 1989; HOLM-HANSEN *et al.*, 1989), the initial nitrate concentration ($[\text{NO}_3]_i$) was 30 mmol m^{-3} (HOLM-HANSEN *et al.*, 1977) and the pre-bloom chlorophyll concentration was 0.1 mg m^{-3} (CLARKE *et al.*, 1988; BRIGHTMAN and SMITH, 1989). Maximum specific growth rates predicted by the model were 0.42 day^{-1} , which is in good agreement with estimates in the literature (WILSON *et al.*, 1986; SAKSHAUG and HOLM-HANSEN, 1986; TILZER and DUBINSKY, 1987; SPIES, 1987). The model is used to predict the final biomass of the phytoplankton crop as Chl *a* at the end of the spring season (summer solstice) for different combinations of mixing depth and losses.

RESULTS AND DISCUSSION

Distribution of physical and biological properties

The seasonal deepening of the UML and its relationship to phytoplankton biomass in the water column is evident in vertical profiles of salinity, temperature and beam transmission for two contrasting stations, Sta. 43 in Gerlache Strait and Sta. 20 in Drake Passage (Fig. 2). The profiles showing per cent beam transmission are indicative of the phytoplankton biomass, as particulate beam attenuation coefficients derived from transmission data in waters with little inorganic sediment have been shown to be proportional to particulate organic carbon concentrations (BISHOP, 1986). In general, values of salinity, temperature (and therefore density) and beam transmission were constant with depth near the surface. The rate of physical mixing in the UML apparently was faster than the rate processes controlling phytoplankton crop size: particles (beam transmission) and pigments were usually constant in the UML. A few exceptions to this rule were noted, including Sta. SA43 (Fig. 2). Such observations were rare and were observed in very calm conditions at stations with high biomass and a shallow UML. Extracted Chl *a* + phaeo concentrations at Sta. 43 ranged from over 50 mg m^{-3} in January to approximately 1.0 mg m^{-3} in March. At Sta. 20 the extracted Chl *a* + phaeo values in surface waters were relatively invariant and ranged from 0.5 to 0.8 mg m^{-3} during the 4 months. Temperature variations in the upper 50 m of the water column between December and March were very pronounced at Sta. 43. In December the upper mixed layer was shallow ($\sim 7 \text{ m}$) and warm (1.8°C). By January the surface water had cooled to 1.4°C , but a temperature maximum of 2.0°C existed at 20 m depth. By March the water column was well mixed to $\sim 38 \text{ m}$, and surface water was close to 0°C . The same trends are seen in the data for Sta. 20. There is a cooling and deepening of the upper mixed layer from January to March.

The salinity data at Sta. 20 show uniform concentrations down to 40, 60 and 65 m during these 3 months. During January, temperature was uniform to only 15 m at Sta. SB20. Thus the Z_{UML} at this perennially low-biomass station was slightly deeper than the 10 m Z_{UML} for Stas SA43 and SB43 in December and January, respectively. In spite of strong seasonal gradients in temperature of the UML, the main factor in stratification was the surface salinity gradient. We believe the weak temperature induced stratification at 15 m observed at SB20 in January to be ephemeral, so that it did not persist for sufficient time for a bloom to develop. It may not be appropriate, therefore, to seek to find a predictive relationship between the phytoplankton crop size and depth of mixing at a single station. However, taking the RACER data set as a whole or using averaging by cruise or region, definite trends between mixing depth and the crop size emerge.

The mean UML for all RACER stations during the months December to March were 15, 17, 26 and 30 m, respectively (Fig. 3). Data in this figure also show phytoplankton Chl *a* concentrations (both in surface waters and when integrated to 50 m depth) during the same time period. It is seen that phytoplankton abundance decreases while Z_{UML} increases simultaneously. During the period from December to February, Chl *a* concentrations (both in surface waters and when integrated to 50 m), decreased by $\sim 80\%$. Solar irradiance also was decreasing during this time period, but data on photosynthesis vs irradiance characteristics of these populations strongly suggest that this phytoplankton decrease in surface waters from January to March cannot be ascribed solely to decreasing irradiance levels (HOLM-HANSEN and MITCHELL, 1991). However, the combination of lower surface irradiance and deeper mixing, resulting in lower mean irradiance of the

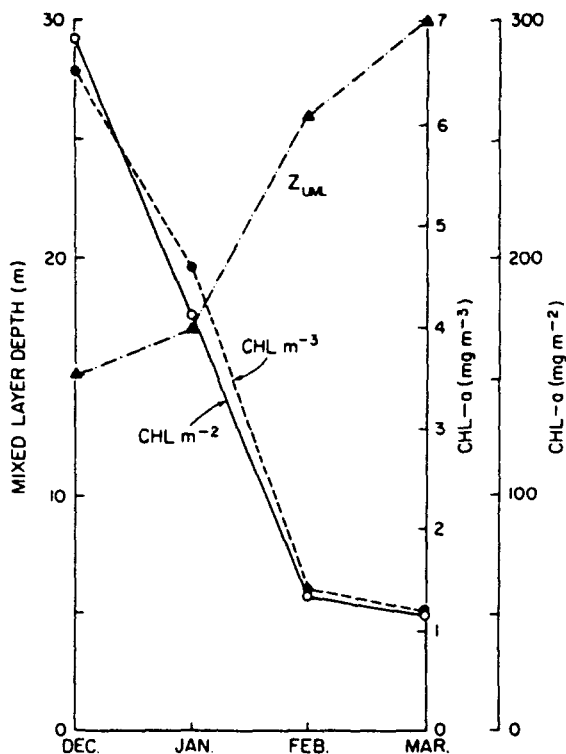


Fig. 3. Plot showing seasonal aspects of depth of the upper mixed layer as related to phytoplankton concentrations (both in surface waters and when integrated to 50 m depth). Values are the mean for all RACER stations from December to March.

UML, may be a factor in the demise of the bloom. Accumulation or decline of the phytoplankton crop will be determined by the relative magnitude of μ and l . As the mean light level in the UML decreases due to lower $PAR(0^+)$ and a deeper Z_{UML} , a rapid decline in the crop would occur if l exceeds μ .

Within the RACER sampling grid, the richest areas in regard to biological production were in or close to Gerlache Strait, while the least productive waters were found at the offshore stations in Drake Passage (HOLM-HANSEN and MITCHELL, 1991). This is illustrated by the data collected during fast cruise C in early February (Fig. 4). The region between Stas 33 and 43 is characterized by high Chl *a* concentrations ($>5.0 \text{ mg Chl } a \text{ m}^{-3}$) with strong stratification in the upper 15 m (and therefore shallow UMLs). Throughout the remainder of the vertical section, Chl *a* concentrations were much lower ($<2 \text{ mg Chl } a \text{ m}^{-3}$ in Bransfield Strait and $<0.5 \text{ mg Chl } a \text{ m}^{-3}$ in Drake Passage) and the upper water column was much less stratified. These dramatic differences within the RACER stations cannot be attributed merely to depth of the bottom (see Fig. 4C). The region between Stas 33 and 43 is fairly shallow (100–200 m), but the region between Stas 37 and 40 is also shallow (bottom depth of 84–200 m), but did not show elevated biomass or marked stratification in water density.

Along the transect in Fig. 4, 85% (S.D. = 6.9%; $n = 12$) of the density change between the UML and 40 m was due to changes in salinity. Although salinity changes dominated stratification throughout, the magnitude of the salinity change was much greater near-

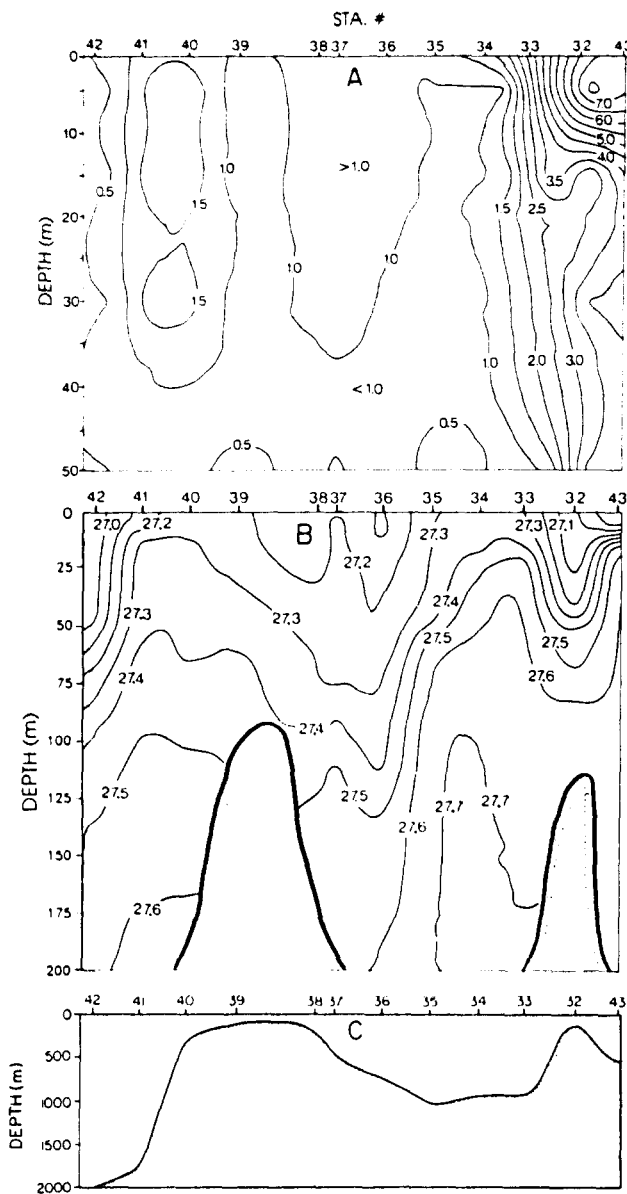


Fig. 4. Vertical section during the "fast" cruise in February 1987 from FC43 in Gerlache Strait to FC42 in Drake Passage, showing the distribution of Chl *a* (mg m^{-3}) from 0 to 50 m (A), the water density (σ_t) from 0 to 200 m (B), and the bottom contour (C).

shore. At Sta. SC43 the change in salinity between the UML and 40 m was 0.86‰ while at Sta. SC42 it was only 5% of this value (0.035‰). During the 1986–87 austral spring/summer, there was very little sea ice in the RACER study region. In fact the only significant sea ice observed during the RACER cruises was offshore during December, and it prevented us from completing the Drake Passage stations off the shelf break during cruise A. Captain Gates of R.V. *Polar Duke* reported that sea ice had been minimal in the

Bransfield and Gerlache Straits since September. What, then, was the source of the fresh water observed nearshore which promoted stratification and shallow UMLs in the southwest portion of the RACER survey? We hypothesize that glacial meltwater from the islands and the Peninsula provided a significant source of fresh water which initiated the stratification leading to favorable light conditions for phytoplankton growth.

Mixing depth and phytoplankton crop during RACER

The concentration of Chl *a* + phaeo in surface waters for 246 RACER stations has been plotted against Z_{UML} (Fig. 5A). The results show that all stations with Chl *a* + phaeo concentrations more than 10 mg m^{-3} had an UML of less than 25 m, while most were less than 20 m. It is also evident, however, that a shallow UML is not always characterized by elevated Chl *a* + phaeo concentration, as many stations with upper mixed layers of less than 20 m showed low pigment concentrations. All stations with deep mixed layers showed consistently low pigment concentrations. Nevertheless, Chl *a* + phaeo values of $1\text{--}2 \text{ mg m}^{-3}$ were observed for a Z_{UML} as deep as 70 m. It is likely that significant amounts of phytoplankton are transported to deep depths by storm-induced deep mixing of stations which had a shallow Z_{UML} with elevated phytoplankton biomass.

A combination of mixing depth and duration of the depth of the UML is essential to predict accumulation of biomass. Unfortunately, the frequency, duration and strength of mixing events are not well known. Nevertheless, the strength of stratification below the UML should provide some index of the persistence of a specific Z_{UML} . One might hypothesize that a scaling parameter which combines mixing depth and the stability of the pycnocline immediately below the UML might provide a better predictor of biomass than the Z_{UML} alone. We define the dimensionless parameter E_{UML} as

$$E_{\text{UML}} = Z_{\text{UML}} \times E_{-75}^{Z_{\text{UML}}}, \quad (7)$$

where Z_{UML} is the depth of the UML and $E_{-75}^{Z_{\text{UML}}}$ is the stability of the water column ($E = -1/\rho \delta\rho/\delta z$; compressibility of seawater is ignored) from the base of the UML to 75 m.

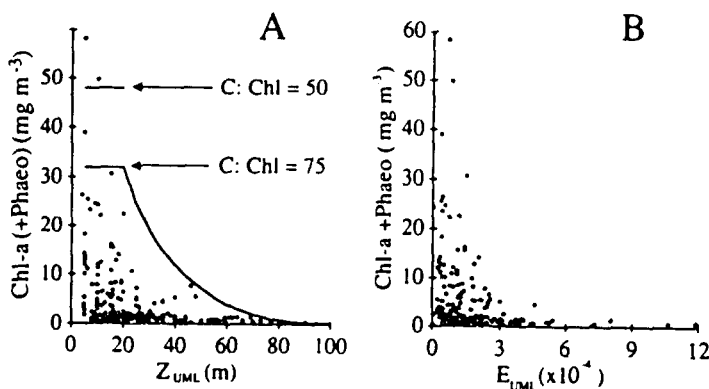


Fig. 5. (A) Concentration of Chl *a* + phaeopigments in surface waters as related to depth of the upper mixed layer. Data shown are from all 69 stations of the RACER grid ($n = 246$). The solid line is the result of the biomass model run for 60 days with $l = 0.1$; C: Chl *a* = 75. Also indicated is the maximal [Chl] for a C: Chl *a* of 50. Note that the model does not explicitly include phaeopigments, hence the parenthetical notation for phaeopigments on the ordinate label. (B) The same data as in (A) but the abscissa is the dimensionless parameter E_{UML} defined in equation (7).

Massive blooms are not observed for values of $E_{UML} > 3 \times 10^{-4}$ (Fig. 5B). As with the relationship of pigments and Z_{UML} (Fig. 5A) only an upper limit can be predicted from the relationships observed for individual stations. Both trends have similar statistical significance (Spearman rank correlation; $r_s \geq 0.9$; $n = 246$; $P \leq 0.001$). Much of the observed variance in the two relationships in Fig. 5A and B is due to shallow mixing during calm conditions for stations which are routinely mixed deeply and have low biomass, and also due to periodic deep mixing during strong storms at stations which typically have strong stratification and have developed blooms.

We also present results of a 60-day run of the model for $l = 0.1$, corresponding to a minimum loss term due only to respiration (TILZER and DUBINSKY, 1987), with grazing and sinking losses equal to zero (Fig. 5A). Only three of 246 stations are above the model result for a C:Chl $a = 75$ (w/w). For this comparison, the maximum concentration of pigment was determined by

$$[\text{Chl } a] \text{ mg m}^{-3} = [\text{NO}_3]_i \times \text{C:N} \times (12 \text{ mg C mmol}^{-1}) \times (\text{C:Chl } a)^{-1}. \quad (8)$$

Thus the system is treated as a nutrient-limited "batch culture" with no vertical transport of nitrogen into the UML which remains at a constant depth during the 60-day run. The fact that observed pigment concentration exceeded 32 mg m^{-3} (the maximum value for C:Chl $a = 75$, C:N = 6.6 and $[\text{NO}_3] = 30$) implies either a requirement of vertical transport of nitrate from below the pycnocline, or a C:Chl a of less than 75. The maximum attainable pigment concentration for a C:Chl a of 50 is indicated for reference; it exceeds the curve for C:Chl a of 75 by a similar factor throughout the depth range (100 m) for which the model is run.

The model is particularly sensitive to the value of C:Chl a chosen as this parameter and the C:N ratio sets the maximum attainable [Chl a] for an initial $[\text{NO}_3]$. When realistic losses in addition to respiration are included, a C:Chl a of 50 provides good agreement to observations (Fig. 6). We believe that a C:Chl a value of 50 is probably typical for Antarctic phytoplankton although values for total particulate organic carbon to Chl a (POC:Chl a) have been reported to be much higher. For example, NELSON *et al.* (1989) have summarized values for POC:Chl a values at Antarctic marginal ice zones ranging from 31 to 138. It is noteworthy that their lowest value is for a November cruise, perhaps early in the season before significant accumulations of detrital carbon had occurred. SAKSHAUG and HOLM-HANSEN (1986) reported values of POC:Chl a ranging from 55 to 132 for natural assemblages and on-deck batch cultures, while HOLM-HANSEN *et al.* (1989) report values as low as 34 during massive blooms which depleted surface nutrients near Anvers Island. Typical values of POC:Chl a from 11 to 46 have been reported by PALMISANO *et al.* (1985) for sea-ice communities whose algae are considered to be extremely shade adapted. It is reasonable to assume that there is both detrital and heterotrophic carbon in natural systems so values at the upper limit of observations (POC:Chl $a > 100$) may be higher than the true C:Chl a of phytoplankton. Using direct microscopic observations for phytoplankton carbon and extracted Chl a , HEWES *et al.* (1990) determined C:Chl a for autotrophs ranging from 50 to 80 for regions where Chl $a > 1 \text{ mg m}^{-3}$, which was typical for most of the RACER observations.

We therefore feel our overall estimate of a C:Chl $a = 50$ for the phytoplankton is reasonable when compared to the range of observations of POC:Chl a (≈ 10 –150) in Antarctic systems. For loss rates of $l = 0.1$ as in Fig. 5A, the model predicts pigment concentrations above most observed concentrations for C:Chl a of 50 or 75. Two factors

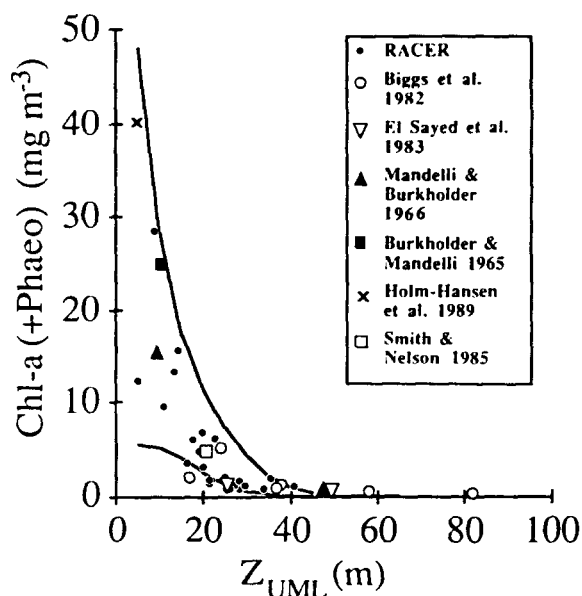


Fig. 6. Concentration of Chl *a* + phaeopigments in surface waters as related to depth of the upper mixed layer. Data for RACER and from HOLM-HANSEN *et al.* (1989) include phaeopigments; other reports and model results are for Chl *a* only, hence the parenthetical notation for phaeopigments on the ordinate label. The solid lines are for model runs where $l = 0.3$ (upper line) and $l = 0.35$ day⁻¹ (lower line). Besides the RACER data which represent mean values for each water mass during each cruise, the data of BIGGS *et al.* (1982) represent mean values for transects or ice-edge stations during the VULCAN Leg 6 cruise and the data of SMITH and NELSON (1985) represent a mean value during an ice-edge bloom in the Ross Sea. All other values are individual observations. All observations were made from December to early February when the maximum summer crop is expected, except data from RACER cruises C and D.

that must be considered in order for the model to provide a predictive capability of the observed biomass are (1) realistic loss rates including grazing and sinking must be included, and (2) observed values for the Z_{UML} at individual stations may not be a good index of the typical Z_{UML} at the same station over the spring season.

Seasonal and spatial variance in Z_{UML} and Chl *a*

Although we assume a constant Z_{UML} during runs of the model, we do not presume that the ecosystem actually exhibits such invariance. The RACER study region was selected because of our expectation that substantially different water masses could be observed through time (HUNTLEY *et al.*, 1991). NILER *et al.* (1991) have defined six separate water masses that maintain some degree of temperature-salinity differentiation (see Fig. 1 for stations included in each mass). It is appropriate to study mean relationships between phytoplankton and mixing for different water masses where the mean environmental forcing may have been different due to proximity (or lack of proximity) to land and/or sources of meltwater (Table 2). Massive blooms (Chl *a* + phaeo > 10 mg m⁻³) were observed in masses IV, V and VI in December (cruise A) but only in mass VI in January (cruise B). No massive blooms were observed in any of the six water masses in February or March. We note that mass I in Drake Passage never developed a bloom (Chl *a* ≥ 1) and

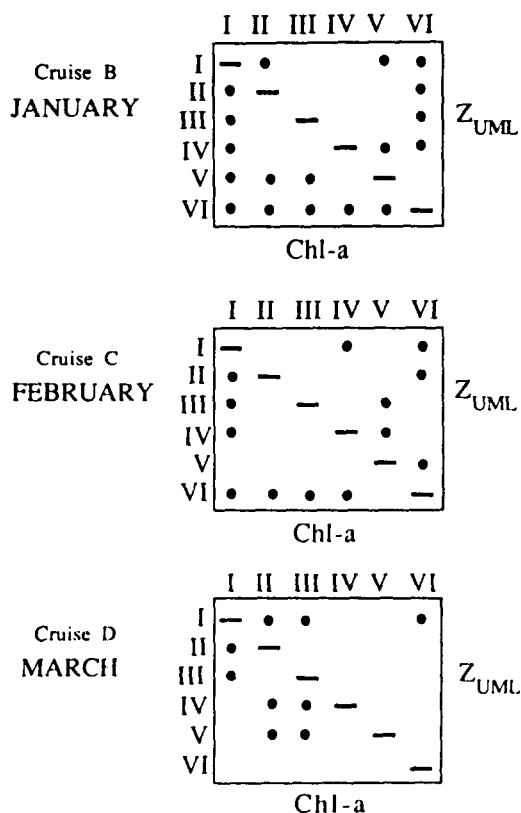
Table 2. Mean values and standard error of the mean (S.E.) for Z_{UML} , Chl *a* (mg m^{-3}) and phaeopigments (mg m^{-3}) for the six water masses described by NILLER et al. (1991) during each of the four RACER cruises. *n* is the number of stations used in each determination. Cruises A, B, C, and D were in December, January, February and March, respectively

Cruise	Mass	<i>n</i>	Z_{UML}		Chl <i>a</i>		Phaeopigments	
			Mean	S.E.	Mean	S.E.	Mean	S.E.
A	I	1	28	—	0.63	—	0.28	—
A	II	9	17	4	4.91	1.05	1.72	0.33
A	III	8	17	3	4.43	0.57	1.70	0.26
A	IV	7	13	3	8.82	1.83	4.04	1.15
A	V	1	5	—	8.43	—	3.93	—
A	VI	8	14	3	11.20	2.13	4.43	0.98
B	I	8	25	4	0.66	0.11	0.26	0.04
B	II	18	16	2	2.44	0.32	1.21	0.24
B	III	9	20	3	2.38	0.28	0.91	0.13
B	IV	7	22	4	3.03	0.91	3.21	1.30
B	V	7	11	4	6.05	1.41	3.46	0.79
B	VI	9	9	2	13.52	2.27	15.01	3.47
C	I	11	34	5	0.60	0.06	0.26	0.04
C	II	23	27	3	1.14	0.09	0.50	0.03
C	III	13	22	4	1.27	0.14	0.53	0.05
C	IV	11	21	3	1.04	0.08	0.41	0.03
C	V	8	35	6	1.35	0.43	0.58	0.17
C	VI	13	19	2	3.43	0.84	1.35	0.33
D	I	9	41	6	0.72	0.11	0.38	0.04
D	II	21	21	2	1.35	0.11	0.54	0.03
D	III	14	28	3	1.16	0.07	0.53	0.04
D	IV	12	30	4	0.79	0.07	0.41	0.03
D	V	6	26	6	0.58	0.04	0.33	0.03
D	VI	13	25	4	1.66	0.38	0.62	0.15

that observed Chl *a* for the other water masses reached their peak in late December. This timing of the peak bloom justifies our termination of the biomass model at the summer solstice. In mass VI Chl *a* was slightly higher in January compared to December, but not significantly so. Phaeopigments increased significantly in mass VI from December to January, presumably due to grazing.

A statistical test of the difference between mean values of Z_{UML} and Chl *a* for the different masses during January, February and March is presented in Table 3. No comparison of means is presented for December as two masses had only one observation (Table 2). In January the Z_{UML} of mass VI (9 m) was significantly shallower than the Z_{UML} for all masses except mass V (11 m). Mass I had the deepest Z_{UML} (25 m) but this was not significantly different than the Z_{UML} of masses III and IV (20 and 22 m, respectively). Concentrations of Chl *a* for masses I and VI were significantly different than Chl *a* concentrations of each of the other masses in January, with mass I being lower and mass VI being higher than all other masses. This statistical analysis supports the RACER hypothesis that conditions nearshore are unique in providing an environment conducive to rich phytoplankton blooms. In February, the offshore-onshore gradient in pigments still indicated that masses I and VI were unique but differentiation in Z_{UML} is less. Less

Table 3. Results of an analysis to test the significance of the difference between mean values of Z_{UML} and Chl *a* for each region during each cruise from January to March. The December cruise is not included because two regions had only one value due to ice cover or mechanical problems. The regions which are significantly different from each other ($P < 0.05$; Student's *t*-test between mean values) are indicated with (●) in the matrices. The upper half of each matrix tests mean values for Z_{UML} , the lower half Chl *a*



differentiation in Z_{UML} is expected as the UML deepens throughout the study region. Regions that had accumulated high biomass earlier in the season may still have had elevated biomass even though it may have been reduced due to dilution as mixing occurs. By March, masses II and III near the South Shetland Islands tend to exhibit the most statistical differentiation in pigments and mixing depths. Although mass VI still had the highest mean Chl *a* in March (1.66), the range in Chl *a* for this region is large (0.2–5 mg Chl *a* m^{-3}) and has a high standard error. We believe the factors which make the coastal waters of Gerlache Strait unique for promoting and sustaining massive blooms in spring and summer are no longer present by March. In autumn, meltwater would be reduced due to colder temperatures and lower insolation and storms would be more frequent and more intense. We propose that both a proximity to meltwater from glaciers and abundant icebergs in the coastal region, and reduced wind mixing due to moderation of storms by land masses contributed to the unique ability for mass VI to develop massive blooms by December and sustain them through January.

Strength of stratification and wind mixing

The susceptibility to wind-induced deepening of the UML is related to the strength of stratification below the UML. When the biomass model is run with realistic loss terms (see Fig. 6, discussion below) it is evident that blooms ($\text{Chl } a > 1 \text{ mg m}^{-3}$) do not develop for a UML $> 40 \text{ m}$. Thus it is of interest to compare, using the same objective criterion, the wind speeds which would be required to mix the various density profiles we observed during RACER. For a simple case where there is no net horizontal advection and no net heat flux, the wind energy (and hence wind speed) required to mix a water column to some desired depth can be estimated. Although there are numerous assumptions in the procedure outlined below, it is instructive to evaluate the relative susceptibility to wind mixing for a region such as the RACER study site where strong horizontal gradients in stability were noted.

One may write an energy balance with respect to time for a one-dimensional stratified fluid where surface wind stress is the only source of change in the system's potential energy

$$\delta/\delta t PE = \rho_0 m_0 U_*^3, \quad (9)$$

where PE , ρ_0 , and U_* are the potential energy of the water column, the density of seawater and the friction velocity, respectively (e.g. KRAUS and TURNER, 1967; DENMAN, 1973; NIILER, 1975; NIILER and KRAUS, 1977). The parameter m_0 is a mixing efficiency coefficient and has been determined experimentally to be approximately 1.0 (DAVIS *et al.*, 1981). The left side of the equation is the rate of change in potential energy and can be calculated as the difference between the potential energy after and before a mixing event divided by the duration of the mixing event (DENMAN and MIYAKE, 1973). The potential energy of the water column of interest is dependent on the depth distribution of density (e.g. POND and PICARD, 1978)

$$PE = g \int_{z_B}^0 \rho(z)(z - z_B) dz. \quad (10)$$

For the analyses discussed below, we integrated from a reference depth ($z_B = -70 \text{ m}$) to the surface (0 m). From equation (10) the change in potential energy before and after a hypothetical mixing event can be calculated. Given the time over which this event occurs, equation (9) can be used to determine how strong a wind event would be necessary to cause such a mixing event. Surface wind speed (U_{wind}) is directly proportional to U_*

$$U_{\text{wind}} = U_* (\rho_a/\rho_0)^{-1/2} (C_d)^{-1/2}, \quad (11)$$

where ρ_a is the density of air and C_d is the drag coefficient of the air–water interface. We used a value of $\rho_a = 1.3 \times 10^{-3} \text{ g cm}^{-3}$ which is typical of cold humid air and a value of $C_d = 1.5 \times 10^{-3}$ which is typical for moderate wind speeds (DENMAN and MIYAKE, 1973; NIILER, 1975). The values of the PE increase, and the corresponding sustained wind speed, required to uniformly mix to 40 m the five rate-process stations during RACER cruise B in January are presented in Table 4. This hypothetical mixing scenario is reasonable as the Z_{UML} of Sta. 43 was observed to deepen from 10 m in February to $> 30 \text{ m}$ in March, and the salinity profiles at Sta. 20 were always uniform to at least 40 m although temperature stratification sometimes resulted in a shallower Z_{UML} (Fig. 2). Sustained winds of 10 m s^{-1} over 3 days would be required to mix Stas SB43 and SB48 to 40 m (Table 4). The highest

Table 4. Estimated potential energy change (δPE) for uniform mixing to 40 m from initial conditions observed during the slow cruise in January (cruise SB). Initial conditions for temperature and salinity for Stas SB20 and SB43 are presented in Fig. 2. Also presented are the sustained winds ($m s^{-1}$) which would be required over the period indicated (1–15 days) in order to accomplish this change in water column potential energy

Station	δPE ($10^5 g s^{-2}$)	Duration of sustained winds				
		1 Day	3 Days	5 Days	10 Days	15 Days
SB13	1.8	9.2	6.4	5.4	4.3	3.7
SB20	1.1	7.7	5.4	4.5	3.6	3.2
SB39	0.1	3.1	2.1	1.8	1.4	1.3
SB43	5.7	13.4	9.3	7.9	6.3	5.5
SB48	5.6	13.3	9.3	7.8	6.2	5.4

sustained winds observed during RACER were approximately $15 m s^{-1}$ but lasted less than 24 h (T. Amos, personal communication). Typical conditions in Gerlache Strait during RACER were very calm. Even during storm events, Brabant Island provided a wind block for Sta. 43 and for much of mass VI. Evidently the nearshore stations are adjacent to sources of fresh water during spring and summer which will tend to re-stratify those regions after mixing events. Thus it appears unlikely that those regions would be routinely mixed to depths as great as 40 m as long as fresh water is available. By contrast, Stas SB39 and SB20 would mix to 40 m with single-day wind events of only 3 and $8 m s^{-1}$, respectively.

The open waters of Drake Passage are unprotected from storms and do not have nearby sources of fresh water. Therefore one expects that this region is routinely mixed to 40 m or greater. The vertical profile of Sta. SB20 in January indicates a strong thermo- and halocline at 40 m although the Z_{UML} is $< 15 m$ due to a small temperature change of $0.25^\circ C$ between 15 and 30 m. The structure of this station suggests weak thermal stratification occurring between mixing events which routinely deepen the Z_{UML} at least to the halocline at 40 m. If this interpretation is true, then regular mixing to depths greater than 40 m would prevent the development of blooms as the stratification would not persist for sufficient time for the crop size to increase.

Applications of the biomass model

The mean pigment concentrations and Z_{UML} for each water mass during each cruise were analysed together with reports from the literature from diverse Antarctic Ocean ecosystems in order to determine the generality of the mixing depth–biomass concept outlined in this paper. The data and the model suggest that Antarctic phytoplankton biomass sustains mean specific loss rates of between 0.3 and $0.35 day^{-1}$ with the implicit assumption of no nutrient limitation (Fig. 6). With the loss rate term set equal to respiration only ($0.1 day^{-1}$) the model predicts that massive blooms will form in 60 days for a $Z_{UML} = 65 m$ and $C:Chl a = 50$ or for a $Z_{UML} = 45 m$ and $C:Chl a = 75 m$ (Fig. 5A). To our knowledge, such high Chl *a* in deeply mixed water columns have not been reported for Antarctic waters, so loss rates must be higher or nutrient flux to the UML (including trace metals) must limit the crop size. The apparent minimal total loss term of $0.3 day^{-1}$, which

provides a good upper bound of Antarctic observations (Fig. 6), predicts that blooms of $1 \text{ mg Chl } a \text{ m}^{-3}$ will form for $Z_{\text{UML}} = 40 \text{ m}$ and that massive blooms of $10 \text{ mg Chl } a \text{ m}^{-3}$ will form for $Z_{\text{UML}} = 25 \text{ m}$. Stations SB20 Chl a + phaeo ranged from 0.4 to 0.8 mg m^{-3} , which, according to the model, would indicate a typical Z_{UML} of 45 – 55 m . Although the Z_{UML} was observed to be $<40 \text{ m}$ due to weak temperature stratification, the halocline was always $\geq 40 \text{ m}$ (Fig. 2) and probably defined the depth of routine mixing during storms.

We feel that the light-dependent growth rate component is the best described aspect of the model and is well supported by independent data in the literature. The loss terms are poorly understood and under-described. Of the loss terms, respiration rates probably are easiest to parameterize since we do not expect large seasonal changes in this term. Sedimentation and grazing losses are expected to have tremendous seasonal variations due to life history strategies of zooplankton and phytoplankton. It is probable that specific respiration rates (r) at the low temperatures of the Antarctic are of the order of 0.05 – 0.1 (e.g. TILZER and DUBINSKY, 1987; SAKSHAUG *et al.*, 1991) so that sinking and grazing must comprise approximately 0.2 – 0.25 day^{-1} .

The specific sinking rates for Chl a ($s_{\text{Chl } a}$), carbon (s_c) and primary production (s_p) were estimated for rate-process stations during RACER (Table 5). The mean value of s_p for all stations (excluding SC39 and SD39) was 0.24 day^{-1} which greatly overestimates s since the daily amount of photosynthetic carbon fixed is generally only 2 – 10% of the particulate organic carbon present in the upper 100 m . As indicated in Table 5, Stas SC39 and SD39 were excluded from the evaluation of specific sinking rates in RACER. For these stations, carbon flux exceeded observed production by as much as 200% . High concentrations of inorganic particulates derived either from resuspension from the shallow bottom or from glacial activity on nearby Livingston Island are presumed to be the source of the material. We believe these materials accelerate sedimentation of carbon, perhaps by adsorbing dissolved organic carbon. Resuspended particulate organic carbon from the shallow bottom also may lead to anomalously high flux for these stations. It is therefore inappropriate to bias mean sinking rate estimates for interpretation of Antarctic Ocean ecosystems which are not influenced by such phenomena.

Early in the season, before significant zooplankton stocks are present and before any mass sedimentation of resting spores of phytoplankton, s_p may be a reasonable upper limit of s for phytoplankton. The value for s_p in December (0.07) was much lower than the value of the overall mean or the individual means for January to March. We hypothesize that a healthy phytoplankton crop has values of s_p similar to the observations of December, which would agree with direct observations of phytoplankton settling velocities (JOHNSON and SMITH, 1986). The accelerated rates of sinking later in the season may arise from sinking of fecal material derived from grazers whose population lagged the phytoplankton bloom in addition to cell sinking (KARL *et al.*, 1991). Thus a significant fraction of the s_p calculated in Table 5 may actually be an index of grazing activity. KARL *et al.* (1991) have noted that a significant fraction of sedimenting matter later in the RACER study was amorphous marine snow and fecal pellets of krill. These observations are consistent with those of DUNBAR (1984), VON BODUNGEN *et al.* (1986) and WEFER *et al.* (1988), who reported a dominance of krill fecal matter in their sediment trap samples collected in Bransfield Strait.

At eight stations in December and January, we made direct estimates of the flux rate of Chl a at 100 m . The mean daily flux of Chl a was less than 1% of the 0 – 100 m integrated stock of Chl a and corresponds to a specific sinking rate of $s_{\text{Chl } a} = 0.008$. KARL *et al.* (1991)

Table 5. Observed stock of Chl *a* and phaeopigments, integrated primary production (from HOLM-HANSEN and MITCHELL, 1991), the daily flux at 100 m of organic carbon (from KARL *et al.*, 1991) and Chl *a* at RACER stations. The flux as a per cent of the estimated stock of carbon, the observed stock of Chl *a* and observed production are used to calculate specific daily sinking rates according to: $s = -\ln(1 - (\text{flux}/\text{stock}))$. These specific rates are symbolized as s_c , $s_{chl\ a}$ and s_p for carbon, Chl *a* and production, respectively. Values of s_c and $s_{chl\ a}$ are probably minimum estimates of specific sinking rates of phytoplankton, while values of s_p are considered to be maximal estimates

Month Station	Σ 0-100 m			Prod			100 m Flux			Flux (%)			Specific sinking		
	Chl <i>a</i> (mg m ⁻²)	Phaeo (mg m ⁻²)	Carbon (g m ⁻² day ⁻¹)	Carbon (g m ⁻² day ⁻¹)	Carbon (g m ⁻² day ⁻¹)	Chl <i>a</i> (mg m ⁻² day ⁻¹)	Carbon (g m ⁻² day ⁻¹)	Chl <i>a</i> (mg m ⁻² day ⁻¹)	Carbon (g m ⁻² day ⁻¹)	Chl <i>a</i> Crop*	Carbon Crop	Carbon Prod.	Carbon s_c	Chl <i>a</i> $s_{chl\ a}$	C Prod. s_p
December															
43	742	347	1.95	0.86	0.37	1.08	0.14	1.08	0.12	0.15	0.15	7.0	0.0012	0.0015	0.0723
13	420	175	1.85	1.39	0.19	7.49	0.21	7.49	0.35	1.78	1.78	11.3	0.0035	0.0180	0.1199
48	252	111	3.44	1.06	0.25	0.84	0.11	0.84	0.31	0.33	0.33	3.2	0.0031	0.0033	0.0328
39	267	74	1.70	0.24	0.10	0.51	0.09	0.51	0.26	0.19	0.19	5.1	0.0026	0.0019	0.0525
Dec. mean	420	177	2.23	0.79	0.20	2.48	0.14	2.48	0.26	0.61	0.61	6.7	0.0026	0.0062	0.0694
January															
43	418	386	0.86	0.86	0.37	7.69	0.37	7.69	0.46	1.84	1.84	43.4	0.0047	0.0186	0.5687
13	289	109	1.39	1.39	0.19	5.13	0.19	5.13	0.47	1.77	1.77	13.5	0.0047	0.0179	0.1453
48	247	215	1.06	1.06	0.25	N.D.	0.25	N.D.	0.54	N.D.	N.D.	23.7	0.0054	N.D.	0.2702
39	66	61	0.24	0.24	0.10	0.60	0.10	0.60	0.80	0.91	0.91	42.5	0.0081	0.0091	0.5534
20	46	26	0.41	0.41	0.10	0.13	0.10	0.13	1.33	0.28	0.28	23.4	0.0134	0.0028	0.2668
Jan. mean	213	159	0.79	0.79	0.20	2.71	0.20	2.71	0.72	0.96	0.96	29.3	0.0073	0.0097	0.3609
February															
43	368	150	0.69	0.69	0.20	N.D.	0.20	N.D.	0.39	N.D.	N.D.	29.6	0.0039	N.D.	0.3505
13	82	36	0.39	0.39	0.25	N.D.	0.25	N.D.	2.13	N.D.	N.D.	64.4	0.0215	N.D.	1.0317
48	49	23	0.39	0.39	0.11	N.D.	0.11	N.D.	1.50	N.D.	N.D.	27.7	0.0151	N.D.	0.3242
39	39	27	0.11	0.11	0.12	N.D.	0.12	N.D.	1.88	N.D.	N.D.	112.7	0.0190	N.D.	†
20	44	27	0.40	0.40	0.04	N.D.	0.04	N.D.	0.58	N.D.	N.D.	10.3	0.0058	N.D.	0.1081
Feb. mean	116	53	0.40	0.40	0.15	N.D.	0.15	N.D.	1.30	N.D.	N.D.	48.9	0.0131	N.D.	0.3629
March															
43	42	24	0.18	0.18	0.04	N.D.	0.04	N.D.	0.55	N.D.	N.D.	20.0	0.0055	N.D.	0.2231
48	45	15	0.19	0.19	0.04	N.D.	0.04	N.D.	0.60	N.D.	N.D.	18.9	0.0060	N.D.	0.2101
39	40	39	0.07	0.07	0.15	N.D.	0.15	N.D.	1.89	N.D.	N.D.	212.9	0.0190	N.D.	†
20	32	21	0.21	0.21	0.04	N.D.	0.04	N.D.	0.77	N.D.	N.D.	19.5	0.0078	N.D.	0.2172
March mean	40	25	0.16	0.16	0.07	N.D.	0.07	N.D.	0.95	N.D.	N.D.	40.3	0.0096	N.D.	0.1626
Overall mean	197	103	0.90	0.90	0.14	2.59	0.14	2.59	0.81	0.79	0.79	31.3	0.0081	0.0079	0.2389

*We assume the total POC:(Chl *a* + phaeo) = 100 for estimates of the total carbon crop from Chl *a* + phaeo.

†Stations SC39 and SD39 were not used in the analysis of s_p as extreme concentrations of inorganic sediments were observed at these stations (KARL *et al.*, 1991; MITCHELL and HOLM-HANSEN, 1991) and the ratio of flux/production was >1.0.

report similar low rates of specific flux of ATP and DNA for the same trap deployments. We estimated the integrated stock of POC from 0 to 100 m using Chl *a* + phaeo by assuming a POC:(Chl *a* + phaeo) ratio of 100. Using this conversion it was possible to estimate s_c for all 18 trap deployments. We observed flux of carbon as a per cent of the POC stock ranging from 0.1 to 2% with a mean rate of 0.8%. In general POC sedimentation rates from the euphotic zone in polar regions range from 0.5 to 7% (VON BODUNGEN *et al.*, 1986; VON BODUNGEN, 1986; WASSMAN *et al.*, 1990). In Bransfield Strait, VON BODUNGEN *et al.* (1986) reported a mean rate for POC flux at 100 m of 2.7% of the stock, and their highest rate of 7% was slightly less than the mean increase of the POC crop by primary production. With total production exceeding the rate of sedimentation losses, either nitrate-based production must be a small fraction of total production, or grazing must be more significant than reported.

Assuming nutrients are not limiting, our model indicates that the total specific loss rate of phytoplankton must be approximately 0.3 day^{-1} , and half of that must be grazing as it is evident that the sum of respiration and sinking comprise no more than 0.15 day^{-1} . The model can be used together with information of respiration and sedimentation to estimate the available organic carbon for grazers. One can calculate the carbon production lost due to grazing (P_g)

$$P_g = [\text{Chl } a] C:\text{Chl } a (1 - \exp(-g_z t)). \quad (12)$$

Assuming $[\text{Chl } a] = 5 \text{ mg m}^{-3}$, $C:\text{Chl } a = 50$, $t = 1 \text{ day}$, and $g_z = 0.15 \text{ day}^{-1}$, then daily grazing loss in the mixed layer only would be $\approx 0.7 \text{ g C m}^{-2}$ for $Z_{\text{UML}} = 20 \text{ m}$. Depending on the stock of phytoplankton assumed, the model requires grazing rates 2–10 times higher than rates estimated by HUNTLEY *et al.* (1991) using data of zooplankton biomass collected with a $333 \mu\text{m}$ net during RACER.

The procedures of HUNTLEY *et al.* (1991) undersampled adult krill, and did not sample zooplankton smaller $333 \mu\text{m}$, including crustacean nauplii and protozooplankton. Although it is reasonable to revise their estimates upward due to undersampling of grazers, it is unlikely that any revisions of macrozooplankton grazing would be sufficient to satisfy the model under conditions that nutrients do not limit the total crop size. Alternatively, microzooplankton grazing may be a significant and unresolved component limiting crop size. FROST (1987) concluded that microzooplankton must be a dominant loss term limiting the crop in the subarctic North Pacific where the phytoplankton crop is small although shallow mixed layers and high macronutrients occur in the summer (but see also MARTIN and FITZWATER, 1988). TAYLOR and HABERSTROH (1988) did limited studies during RACER on the role of microzooplankton in the post-bloom period (February to March) and determined that protozooplankton may account for significant grazing. Unfortunately, routine experiments and determinations of abundances during RACER were not done so it is difficult to extrapolate to a general conclusion. Certainly, the data of HEWES *et al.* (1985, 1990) and those of TAYLOR and HABERSTROH (1988) implicate microzooplankton as an important and poorly resolved loss term. On the other hand, VON BODUNGEN *et al.* (1986) and HOLM-HANSEN *et al.* (1989) reported negligible protozooplankton biomass in the eastern Bransfield Strait, and near Anvers Island, respectively.

Vertical diffusion of nutrients predicted by the model

One surprising aspect of the model is the prediction that substantial vertical diffusion of nutrients across the pycnocline must occur in order to develop and sustain massive blooms.

Vertical diffusion is parameterized as an "eddy diffusivity coefficient" which for our purposes is calculated based on the nitrate balance and vertical gradient during the 60-day run of the model

$$k_z = (\text{mmol NO}_3 \text{ m}^{-2} \text{ s}^{-1})(d[\text{NO}_3]/dz)^{-1}. \quad (13)$$

The first term on the right is the mean rate of NO_3 flux into the UML calculated as the total nitrogen fixed during the 60-day run, less the $[\text{NO}_3]_i$, and less the fraction attributed to recycling. The second term is the vertical gradient in nitrate. $d[\text{NO}_3]$ was defined as $[\text{NO}_3]_{50} - [\text{NO}_3]_{\text{UML}}$, the difference in NO_3 concentrations at 50 m and in the UML. dz is calculated as $50 - Z_{\text{UML}}$, the distance from the base of the UML to 50 m. Once the bloom was developed and NO_3 was depleted, $d\text{NO}_3/dz$ was typically about $0.5\text{--}2 \text{ mmol NO}_3 \text{ m}^{-4}$.

As an example, for a 20 m Z_{UML} , a final Chl $a > 10 \text{ mg m}^{-3}$ will be attained after 60 days for $C:\text{Chl } a = 50$ and $l = 0.3$. To develop this bloom, the model predicts that approximately $600 \text{ mmol NO}_3 \text{ m}^{-2}$ must be transported into the UML if 33% of the primary production is based on recycled ammonium. This flux could be supported by a mean k_z of approximately $6 \times 10^{-5} \text{ m}^2 \text{ s}^{-1}$. The value of k_z is approximately $1 \times 10^{-5} \text{ m}^2 \text{ s}^{-1}$ for the same conditions if 67% of the primary production is based on recycled nutrients. A mean value of $k_z = 5 \times 10^{-5} \text{ m}^2 \text{ s}^{-1}$ is determined for all runs of the model for Z_{UML} shallow enough to develop a massive bloom with $l = 0.3$ and percentages of recycling of either 33 or 67%. These two estimates of the fraction of primary production based on recycled nutrients are the extremes of observations reported for the Antarctic Ocean (OLSON, 1980; GLIBERT *et al.*, 1982; RÖNNER *et al.*, 1983; KOIKE *et al.*, 1986; NELSON and SMITH, 1986). These values of k_z are typical for a stratified upper ocean with moderate wind stress (DENMAN and GARGETT, 1983; LEWIS *et al.*, 1986; GREGG, 1987). Thus, nutrient supply across the pycnocline should be adequate provided total loss of the crop averages approximately 0.3 day^{-1} . As discussed above, such loss rates would require higher grazing rates than previously estimated.

Vertical transport of nutrients into the UML should be balanced by the downward transport of particle-rich, nutrient-poor water to depth. As noted by HOLM-HANSEN and MITCHELL (1991), significant phytoplankton biomass was observed below the pycnocline at depths where light was insufficient for net photosynthesis. This deep biomass was generally associated with $[\text{NO}_3]$ below winter-time levels to depths up to 100 m. These observations corroborate our hypothesis of significant vertical transport.

An argument for nutrient limitation of crop size

The current model does not include nutrient limitation of maximal growth rates or of the maximal crop but assumes that the sum of initial concentrations and diapycnal transport of nutrients are adequate to supply the demand of the growing crop. Using this assumption we fit the model to observations (Fig. 6) by parameterizing the total specific loss rate, which we feel is the least known aspect of the model. As discussed above, g_z must be approximately 0.15 day^{-1} to satisfy the requirement that the total value of l must be $\approx 0.3\text{--}0.35 \text{ day}^{-1}$. With loss rates of this magnitude, reasonable values of k_z are required to develop and sustain observed blooms. In general, it is considered that such high grazing rates are not observed on the basis of zooplankton stock size (e.g. SCHNACK *et al.*, 1985; HUNTLEY *et al.*, 1991) or rates of sedimentation of fecal material (e.g. VON BODUNGEN *et al.*, 1986). If grazing rates (and total loss rates) are reduced (i.e. $l = 0.2 \text{ day}^{-1}$) predicted

biomass exceeds observations and values of k_z become unreasonably large (e.g. $k_z = 2 \times 10^{-4} \text{ m}^2 \text{ s}^{-1}$; UML = 20 m; 50% recycled production). The model implies either grazing is much greater than previously estimated, or rates of nutrient supply across the pycnocline limit the rate of biomass accumulation of massive blooms. In the latter scenario, actual specific growth rates need not be limited by nutrients if rates of regeneration are sufficient. High light attenuation coefficients in massive blooms will result in low maximal specific growth rates for phytoplankton in the UML. KOIKE *et al.* (1986) estimated that ammonium provided 72% of the inorganic nitrogen required for coastal phytoplankton even though measured ammonium concentrations were less than 10% ambient nitrate concentrations ($1\text{--}2 \text{ mmol ammonium m}^{-3}$). OLSON (1980) presented data indicating that low concentrations of ammonium ($<0.5 \text{ mmol m}^{-3}$) significantly inhibit the uptake of nitrate. The availability of regenerated nutrients from grazing on the large crop already present is hypothesized to be sufficient to sustain growth rates but not rates of increase of the crop. Once significant ammonium concentrations are established in the UML, nitrate transported across the pycnocline would be used inefficiently. Inefficient nitrate utilization would result in the typical Antarctic observations of high nitrate concentrations ($5\text{--}15 \text{ mmol m}^{-3}$) even in blooms.

CONCLUSIONS

During RACER, highest biomass conditions always had a shallow Z_{UML} , and deep Z_{UML} conditions always had low biomass. Deviation of individual observations from this trend is probably caused by inadequate resolution of the time that the UML has been at a particular depth, and short-term variations in s and g_z , which may undergo extreme spatial and temporal variations. Massive sedimentation of diatom resting spores, or intense grazing by localized krill or salp swarms occur for this ecosystem. The time-scale of mixing stratification and duration of a shallow Z_{UML} is undoubtedly of great importance in Antarctic waters in regard to formation of blooms. The temperature-dependent lag in phytoplankton development limits the extent and duration of blooms in Antarctic waters, as it requires that wind-induced deep mixing of the upper water column be minimal for periods of weeks. Such shelter from storms may only occur for coastal environments or in the lee of islands where storm intensities are abated (e.g. CLARKE *et al.*, 1988). During RACER, stations in and close to Gerlache Strait were normally calmer than offshore stations.

Offshore regions are predicted to have an upper limit to biomass due to inadequate ratios of iron (and perhaps other trace nutrients) relative to the concentrations of macronutrients (MARTIN and FITZWATER, 1988; MARTIN *et al.*, 1990). With no losses due to sinking or grazing, crop size should conform to LIEBIG's (1840) law of the minimum. Demonstration of low iron concentrations alone are not sufficient to declare iron as limiting if the surface layer is routinely mixed to depths that may make light the limiting factor. BUMA *et al.* (1990) report that iron in the Scotia Sea is sufficient to support $[\text{Chl } a] \approx 4 \text{ mg m}^{-3}$ corresponding to a depletion up to 15% of $[\text{NO}_3]$. That region of the Scotia Sea was not observed to have $[\text{Chl } a] > 1 \text{ mg m}^{-3}$ by BIGGS *et al.* (1982; data presented in Fig. 6). Our model assumes nutrients are not limiting. The critical experiment will be to determine if iron (or some other trace element) is reduced to undetectable levels in mid-summer, while macronutrients remain high. If not, then some other factor, perhaps light, may in fact be the limit for these open-ocean regions. Regardless, our model is relevant to

bloom development for coastal zones or ice edges where iron is not expected to be limiting (MARTIN and FITZWATER, 1988; MARTIN *et al.*, 1990).

Our model predicts a relatively high loss due to predation which is higher than generally accepted based on biomass collections of macrozooplankton. Lower grazing rates require unreasonably high values of k_z , and predicted biomass in the UML exceeds observations. We are forced to conclude that one of two paradigms of Antarctic biological oceanography must be revised: either grazers consume a greater fraction of the crop than previously estimated, or rates of nutrient supply to the UML limits the accumulation of biomass in massive blooms. Current data sets are not adequate to resolve whether these hypotheses are reasonable. Both may actually be of importance. Underestimates of grazing, particularly the contribution of protozooplankton, are inherent in the traditional methods of sampling with nets; rates of regeneration and ammonium-based production have not been well documented in massive coastal blooms. Although the role of protozooplankton is poorly understood for the Antarctic, and conflicting reports of their significance are found in the literature, they are presumed to be an important but unresolved component of crop loss.

To address the questions raised here, future studies must be multi-disciplinary. Besides traditional biological rate-process studies, studies of surface and *in situ* irradiance, trace element limitation and microzooplankton grazing are essential. Physical measurements of continuous meteorological conditions and turbulent kinetic energy dissipation are required so that wind stress, its effect on rate and depth of mixing of the upper water column, and rate constants for phytoplankton mixing and nutrient transport can be calculated simultaneously.

Acknowledgements—This work was supported by National Science Foundation Grant DPP-85-19908. We are indebted to the captain and crew of R. V. *Polar Duke*, who were most helpful in all our shipboard operations. We also thank the personnel at Palmer Station for their support of our studies; D. Karl for sediment trap material for Chl *a* flux analysis; D. Menzies and T. Amos for valuable work both during and after the cruise; P. Niler for helpful suggestions; A. Zirino and H. Sosik and two anonymous reviewers for critical comments on the manuscript; Brian D. Schieber for programming and analysis; and Eric A. Brody and Osmund Holm-Hansen III for computer graphics preparation.

REFERENCES

- AUSTIN R. W. (1974) Inherent spectral radiance signatures of the ocean surface. In: *Ocean color analysis*, SIO Reference 74-10, University of California, San Diego, California, pp. 1–20.
- BIGGS D. C., M. A. JOHNSON, R. R. BIDIGARE, J. D. GUFFY and O. HOLM-HANSEN (1982) Shipboard autoanalyzer studies of nutrient chemistry, 0–200 m, in the eastern Scotia Sea during FIBEX. Technical Report 82-11-T, Department of Oceanography, Texas A&M University, College Station, Texas, 98 pp.
- BISHOP J. K. B. (1986) The correction and suspended matter calibration of Sea Tech transmissometer data. *Deep-Sea Research*, **33**, 121–134.
- BODUNGEN B. VON (1986) Phytoplankton growth and krill grazing during spring in the Bransfield Strait, Antarctica—Implications from sediment trap collections. *Polar Biology*, **6**, 153–160.
- BODUNGEN B. VON, V. SMETACEK, M. M. TILZER and B. ZEITZSCHELL (1986) Primary production and sedimentation during spring in the Antarctic Peninsula region. *Deep-Sea Research*, **33**, 177–194.
- BOYD C. M., M. HEYRAUD and C. N. BOYD (1984) Feeding of the antarctic krill *Euphausia superba*. *Journal of Crustacean Biology*, **4**, Special No. 1, 123–141.
- BRIGHTMAN R. I. and W. O. SMITH (1989) Photosynthesis–irradiance relationships of Antarctic phytoplankton during austral winter. *Marine Ecology Progress Series*, **53**, 143–151.
- BUMA A. G. J., H. R. F. NOLTING, J. W. DE BAAR, G. JACQUES and P. J. TREGUER (1990) Testing the iron limitation hypothesis for phytoplankton from the Southern Ocean. *EOS*, **71**, 67.

- BURKHOLDER P. R. and E. F. MANDELLI (1965) Carbon assimilation of marine phytoplankton in Antarctica. *Proceedings of the National Academy of Science of the USA*, **54**, 437–444.
- CLARKE A., L. J. HOLMES and M. G. WHITE (1988) The annual cycle of temperature, chlorophyll and major nutrients at Signy Island, South Orkney Islands, 1969–82. *British Antarctic Survey Bulletin*, **80**, 65–86.
- DAVIS R. E., R. DESZOEKE and P. NIILER (1981) Variability in the upper ocean during MILE—II. Modeling the mixed layer response. *Deep-Sea Research*, **28**, 1427–1452.
- DENMAN K. L. (1973) A time-dependent model of the upper ocean. *Journal of Physical Oceanography*, **3**, 173–184.
- DENMAN K. L. and M. MIYAKE (1973) Upper layer at ocean station Papa: Observations and simulation. *Journal of Physical Oceanography*, **3**, 185–195.
- DENMAN K. L. and A. E. GARGETT (1983) Time and space scales of vertical mixing and advection of phytoplankton in the upper ocean. *Limnology and Oceanography*, **28**, 801–815.
- DUNBAR R. B. (1984) Sediment trap experiments on the Antarctic continental margin. *Antarctic Journal of the United States*, **19**, 70–71.
- EL-SAYED S. Z. (1987) Biological productivity of Antarctic waters: present paradoxes and emerging paradigms. In: *Antarctic aquatic biology*, S. Z. EL-SAYED and A. P. TOMO, editors, SCAR Cambridge, pp. 1–21.
- EL-SAYED S. Z., D. BIGGS and O. HOLM-HANSEN (1983) Phytoplankton standing crop, primary productivity and near-surface nitrogenous nutrient fields in the Ross Sea, Antarctica. *Deep-Sea Research*, **30**, 1017–1032.
- FROST B. W. (1987) Grazing control of phytoplankton stock in the open subarctic Pacific Ocean: a model assessing the role of mesozooplankton, particularly the large calanoid copepods *Neocalanus* spp. *Marine Ecology Progress Series*, **39**, 49–68.
- GLIBERT P. M., D. BIGGS and J. J. MCCARTHY (1982) Utilization of ammonium and nitrate during austral summer in the Scotia Sea. *Deep-Sea Research*, **29**, 837–850.
- GREGG M. C. (1987) Diapycnal mixing in the thermocline: a review. *Journal of Geophysical Research*, **92**, 5249–5286.
- HART T. J. (1934) On the phytoplankton of the south-west Atlantic and the Bellingshausen Sea. *Discovery Reports*, **8**, 1–286.
- HEWES C. D., E. SAKSHAUG and O. HOLM-HANSEN (1985) Alternative pathways at lower trophic levels in the Antarctic food web. In: *Antarctic nutrient cycles and food webs*, W. R. SIEGFRIED, P. R. CONDY and M. R. LAWS, editors, Springer, Berlin, pp. 277–283.
- HEWES C. D., E. SAKSHAUG, F. M. H. REID and O. HOLM-HANSEN (1990) Microbial autotrophic and heterotrophic eucaryotes in Antarctic waters: Relationships between biomass and chlorophyll, adenosine triphosphate and particulate organic carbon. *Marine Ecology Progress Series*, **63**, 27–35.
- HOLM-HANSEN O. and B. RIEMANN (1978) Chlorophyll *a* determination: improvements in methodology. *Oikos*, **30**, 438–447.
- HOLM-HANSEN O. and B. G. MITCHELL (1991) Spatial and temporal distribution of phytoplankton and primary production in the western Bransfield Strait region. *Deep-Sea Research*, **38**, 961–980.
- HOLM-HANSEN O., C. J. LORENZEN, R. W. HOLMES and J. D. H. STRICKLAND (1965) Fluorometric determination of chlorophyll. *Journal du Conseil International pour l'Exploration de la Mer*, **30**, 3–15.
- HOLM-HANSEN O., S. Z. EL-SAYED, G. A. FRANCESCHINI and R. L. CUHEL (1977) Primary production and the factors controlling phytoplankton growth in the Southern Ocean. In: *Adaptations within antarctic ecosystems*, G. A. LLANO, editor, Gulf, Houston, Texas, pp. 11–50.
- HOLM-HANSEN O., B. G. MITCHELL, C. D. HEWES and D. M. KARL (1989) Phytoplankton blooms in the vicinity of Palmer Station, Antarctica. *Polar Biology*, **10**, 49–57.
- HUNTLEY M., D. M. KARL, P. NIILER and O. HOLM-HANSEN (1991) Research on Antarctic Coastal Ecosystem Rates (RACER): an interdisciplinary field experiment. *Deep-Sea Research*, **38**, 911–941.
- JOHNSON T. O. and W. O. SMITH (1986) Sinking rates of phytoplankton assemblages in the Weddell Sea marginal ice zone. *Marine Ecology Progress Series*, **33**, 131–137.
- KARL D. M., B. D. TILBROOK and G. TIEN (1991) Seasonal coupling of organic matter production and particle flux in the Bransfield Strait, Antarctica. *Deep-Sea Research*, **38**, 1097–1126.
- KOIKE I., O. HOLM-HANSEN and D. C. BIGGS (1986) Inorganic nitrogen metabolism by Antarctic phytoplankton with special reference to ammonium cycling. *Marine Ecology Progress Series*, **30**, 106–116.
- KRAUS E. B. and J. S. TURNER (1967) A one-dimensional model of the seasonal thermocline. Part II. The general theory and its consequences. *Tellus*, **19**, 98–105.
- LEWIS M. R., W. G. HARRISON, N. S. OAKEY, D. HERBERT and T. PLATT (1986) Vertical nitrate fluxes in the oligotrophic ocean. *Science*, **234**, 870–873.

- LIEBIG J. (1840) *Chemistry in its application to agriculture and physiology*. Taylor and Walton, London.
- MANDELLI E. F. and BURKHOLDER (1966) Primary productivity in the Gerlache and Bransfield Straits of Antarctica. *Journal of Marine Research*, **24**, 15–27.
- MARTIN J. H., R. M. GORDON and S. FITZWATER (1990) Iron in Antarctic waters. *Nature*, **345**, 156–158.
- MARTIN J. H. and S. FITZWATER (1988) Iron deficiency limits phytoplankton growth in the north-east Pacific subarctic. *Nature*, **331**, 341–343.
- MITCHELL B. G. and O. HOLM-HANSEN (1991) Bio-optical properties of Antarctic waters: differentiation from temperate ocean models. *Deep-Sea Research*, **38**, 1009–1028.
- MOREL A. (1988) Optical modeling of the upper ocean in relation to its biogenous matter content (Case I waters). *Journal of Geophysical Research*, **93**, 10,749–10,768.
- NELSON D. M. and W. O. SMITH (1986) Phytoplankton bloom dynamics of the western Ross Sea ice edge—II. Mesoscale cycling of nitrogen and silicon. *Deep-Sea Research*, **33**, 1389–1412.
- NELSON D. M., W. O. SMITH, R. D. MUENCH, L. I. GORDON, C. W. SULLIVAN and D. M. HUSBY (1989) Particulate matter and nutrient distribution in the ice-edge zone of the Weddell Sea: relationship to hydrography during later summer. *Deep-Sea Research*, **36**, 191–209.
- NILER P. P. (1975) Deepening of the wind-mixed layer. *Journal of Marine Research*, **33**, 405–422.
- NILER P. P. and E. B. KRAUS (1977) One-dimensional models of the upper ocean. In: *Modelling and prediction of the upper layers of the ocean*, E. B. KRAUS, editor, Pergamon Press, New York, pp. 143–172.
- NILER P. P., J. ILLEMAN and J.-H. HU (in press) Lagrangian drifter observations of surface circulation in the Gerlache and Bransfield Strait. *Antarctic Journal of the United States*.
- NILER P. P., A. AMOS and J.-H. HU (1991) Water masses and 200 m relative geostrophic circulation in the western Bransfield Strait region. *Deep-Sea Research*, **38**, 943–959.
- OLSON R. J. (1980) Nitrate and ammonium uptake in Antarctic waters. *Limnology and Oceanography*, **25**, 1064–1074.
- PALMINIANO A. C., J. B. SOO-HOO and C. W. SULLIVAN (1985) Photosynthesis–irradiance relationships in sea ice microalgae from McMurdo Sound, Antarctica. *Journal of Phycology*, **21**, 341–346.
- PLATT T. and A. D. JASSBY (1976) The relationship between photosynthesis and light for natural assemblages of coastal marine phytoplankton. *Journal of Phycology*, **12**, 421–430.
- POND S. and G. L. PICKARD (1978) *Introductory dynamic oceanography*. Pergamon Press, New York, 241 pp.
- REDFIELD A. C., B. H. KETCHUM and F. A. RICHARDS (1963) The influence of organisms on the composition of sea water. In: *The sea*, Vol. 2, M. N. HILL, editor, Interscience, New York, pp. 26–77.
- RÖNNER U., R. SÖRENNSSON and O. HOLM-HANSEN (1983) Nitrogen assimilation by phytoplankton in the Scotia Sea. *Polar Biology*, **2**, 137–147.
- SAKSHAUG E. and HOLM-HANSEN (1986) Photoadaptation in Antarctic phytoplankton: Variations in growth rate, chemical composition and P versus I curves. *Journal of Plankton Research*, **8**, 459–473.
- SAKSHAUG E., G. JOHNSEN, K. ANDRESEN and M. VERNET (1991) Modeling of light-dependent algal photosynthesis and growth: experiments with the Barents Sea diatoms *Thalassiosira nordenskiöldii* and *Chaetoceros furcellatus*. *Deep-Sea Research*, **38**, 415–430.
- SCHNACK S. B., V. SMETACEK, B. VON BODUNGEN and P. SIEYMANN (1985) Utilization of phytoplankton by copepods in Antarctic waters during spring. In: *Marine biology of polar regions and effects of stress on marine organisms*, J. S. GRAY and M. E. CHRISTIANSEN, editors, Wiley, New York, pp. 65–81.
- SMITH R. C. and K. BAKER (1978) The bio-optical state of ocean waters and remote sensing. *Limnology and Oceanography*, **23**, 247–259.
- SMITH W. O. Jr and D. M. NELSON (1985) Phytoplankton biomass near a receding edge in the Ross Sea. In: *Antarctic nutrient cycles and food webs*, W. R. SIEGFRIED, P. R. CONDY and R. M. LAWS, editors, Springer, Berlin, pp. 70–77.
- SPIES A. (1987) Growth rates of Antarctic marine phytoplankton in the Weddell Sea. *Marine Ecology Progress Series*, **41**, 267–274.
- SVERDRUP H. U. (1953) On conditions for the vernal blooming of phytoplankton. *Journal du Conseil International pour l'Exploration de la Mer*, **18**, 287–295.
- TAYLOR G. T. and P. R. HABERSTROH (1988) Microzooplankton grazing and planktonic production in the Bransfield Strait observed during the RACER program. *Antarctic Journal of the United States*, **23**, 126–128.
- TILZER M. M. and Z. DUBINSKY (1987) Effects of temperature and day length on the mass balance of Antarctic phytoplankton. *Polar Biology*, **7**, 35–42.
- TILZER M. M., B. VON BODUNGEN and V. SMETACEK (1985) Light dependence of phytoplankton photosynthesis in

- the Antarctic: Implications in regulating productivity. In: *Antarctic nutrient cycles and food webs*, W. R. SIEGFRIED, P. R. CONDY and R. M. LAWS, editors. Springer, Berlin, pp. 60–69.
- WASSMAN P., M. VERNET and B. G. MITCHELL (1990) Mass sedimentation of *Phaeocystis pouchetii* in the Barents Sea. *Marine Ecology Progress Series*, **66**, 183–195.
- WEFER G., G. FISHER, D. FUETTERER and R. GERSONDE (1988) Seasonal particle flux in the Bransfield Strait, Antarctica. *Deep-Sea Research*, **35**, 891–898.
- WILSON D. L., W. O. SMITH and D. M. NELSON (1986) Phytoplankton bloom dynamics of the western Ross Sea ice edge I: Primary productivity and species-specific production. *Deep-Sea Research*, **33**, 1375–1387.